*Proc. 20th International Colloquium on Scanning Probe Microscopy*
JJAP Conf. Proc. **1** (2013) 011002


# Expression of Tumor Suppressors PTEN and TP53 in Isogenic Glioblastoma U-251MG Cells Affects Cellular Mechanical Properties – An AFM-based Quantitative Investigation

Alexandre Berquand[1], Hella-Monika Kuhn[2], Andreas Holloschi[2], Jan Mollenhauer[3] and Petra Kioschis[2]

[1]*Bruker Nano GmbH, Oestliche Rheinbrueckenstrasse, Karlsruhe, Germany*

E-mail: alexandre.berquand@bruker-nano.com

[2]*University of Applied Sciences Mannheim, Institute of Molecular and Cell Biology, Mannheim, Germany*
[3]*University of Southern Denmark, Lundbeckfonden Center of Excellence NanoCAN, Institute for Molecular Medicine, Odense C, Denmark*

(Received January 15, 2013)

Glioblastoma is the most common and malign form of brain cancer that is highly resistant to therapy and particularly hard to cure since the blood-barrier is not very permeable to drugs. Moreover, a surgery is always highly risky. Thus, there is a real need to develop technique enabling accurate identification of potentially tumor cells at an early stage. It is getting well established that cancer cells are usually softer than their normal homologues and Atomic Force Microscopy (AFM) has proven itself over the last decade to be a tool of choice to characterize cells mechanical properties. Among the various AFM techniques, Force Spectroscopy (FS), especially Force Volume (FV) is the most commonly used. In the present study, AFM has been used to successfully characterize malignant and modified less malignant forms of glioblastoma U-251MG isogenic cells, using FV and Peak Force Tapping (PFT), a newly released AFM mode. Although both modes are quantitative and easy to use, PFT appears as the most relevant. Benefits and drawbacks of both techniques are discussed.

## 1. Introduction

Force Spectroscopy (FS) is by far the most widely used Atomic Force Microscopy (AFM) mode to extract the samples' mechanical properties. Over the last two decades, Atomic Force Microscopy (AFM) [1] has proven itself to be the tool of choice to investigate the morphology and mechanical properties of living cells, especially since the development of tapping mode [2] and force spectroscopy [3]. The main benefit of that technique is that cells can be observed in near-physiological conditions [4-13]. More specifically, during the last 10 years an increasing number of studies were reported showing that cancer cells and their normal homologues exhibit clearly different mechanical properties [14-16]: for instance, AFM has been used to characterize the ultrastructure of bladder cancer cells [17] or to prove that healthy cells in contrast to breast [18,19] and prostate [20] cancer cells show different mechanical properties. Similar differences in elasticity have also been found between normal lymphocytes and leukemia–derived Jurkat cells [21,22]. Actually it is getting well accepted that in response to a force stimulation, cancer cells are usually softer than their counterparts, especially in the case of bladder [23], prostate [20], breast [24], cartilage [25], blood [26] and ovarian [27] tissues. Furthermore, different states of cancer progression for esophageal cells have successfully been correlated to characteristic mechanical properties: normal squamous cells are stiffer than metaplastic cells, and themselves stiffer than their dysplastic homologues [13]. This change in stiffness can be directly associated to a decrease in the actin level in the cell cytoskeleton [28].

All those studies tend to prompt that AFM might become a diagnosis tool for cancer detection [29] and are for the vast majority based on force volume experiments. This technique allows extraction of (among others) stiffness from the measurement but suffers from a lack of resolution and the fact that data have to be post-processed to calculate the Young's modulus. Moreover most of the works mentioned above use a Hertzian [30] fit to represent the contact between the tip and the surface which presents the advantage of neglecting the adhesion forces between the indenter and the sample but has a variety of limitations for the use with biological samples.

The present study aims at showing that a new AFM-based technique called Peak Force Tapping (PFT) can be applied for quantitative measurements of living glioblastoma U-251MG cells for determining the effect of tumor-related genes on biomechanical properties. Glioblastoma multiforme (GBM) is the most lethal primary brain tumor [31]. Drug treatments are without notable success for glioblastomas and despite continuous improvement of GMB therapy, usually consisting in surgical tissue resection, the majority of patients do not survive beyond one year after diagnosis of recurrent disease [32]. Thus, the development of new routine techniques allowing the selective identification of potentially precancerous changes as well as cancerous cells is still a key requirement and an unprecedented technical challenge in order to improve the diagnostic and therapeutic outcomes.
The principle of PFT technique is described in detail in figure 1.

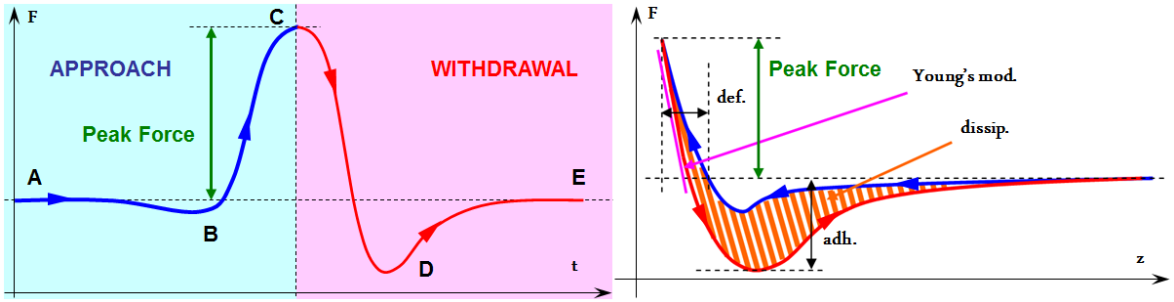


**Fig. 1.** The principle of Peak Force Tapping. Left: representation of the force fields exercised on the AFM cantilever over the time during one approach (in blue)-retract (in red) cycle. First the tip is not subject to any force when far off the surface (A). Then, as approaching the sample surface, it goes through an attractive field first until it reaches out to the contact point (B). Then it indents into the sample until a maximum (C). The vertical distance between the base line and C is referred to as the Peak Force and is used for the feedback calculation. Afterwards, the tips start pulling off (maximum adhesion point in D) to eventually reach back to its original position (E). Right: force vs tip-sample separation distance representation. Such force curve is generated for each pixel of the image, so that simultaneously to the height profile, five different signals can be extracted from these force curves. Abbreviations: def. = deformation, Young's mod. = Young's modulus, dissip. = dissipation and adh. = adhesion. If the AFM probe I calibrated on a standard sample prior to the experiment, all the above information will be displayed in quantitative values.

The probe is oscillated at a drive frequency of 1 kHz and each time it contacts the surface, a force curve is recorded from which several parameters like topography, adhesion, dissipation, deformation and the Young's modulus can be calculated. If the probe is calibrated prior to the experiment on a known material, all those parameters will be directly displayed quantitatively. The speed of image acquisition is similar to tapping mode and the resolution achieved for all channels is identical to the topographical channel. Up to now, PFT had mainly been used to probe the mechanical properties of β-amyloid fibrils [33], fixed cells [34] or living diatoms [35] but has not

yet been thoroughly tested on a wide range of eukaryotic or human cells. Recently, this technique was used to probe the effect of glyphosate, a herbicide thought to induce severe impairments on human skin, on the morphology and mechanical properties of living HaCat cells [36] and proved that this drug can induce a spectacular stiffening on the cells, correlated to the presence of stress fibrils.
In the present work, we used a similar approach to assess if this new AFM mode can be used to evaluate the biological effects of cancer-related candidate genes on mechanical properties of living cells. In the experimental setting, we have analyzed glioblastoma U251-MG cells with induced expression of either wild type tumor suppressor PTEN or TP53, respectively, in comparison with non-modified U251-MG glioblastoma cells in which the two tumor suppressor genes are inactivated shifting cells to a more tumorigenic state. We hereby report an AFM-based study where FV and PFT have been quantitatively used to examine the impact of genetic modifications on mechanical properties of isogenic glioblastoma cell lines, and to test the potential of this method to discriminate between cells with different tumorigenic behaviour.

## 2. Material and Methods

- **Cell lines and cell culture:** Isogenic glioblastoma U-251MG cell lines were constructed using a site-specific recombination-based strategy combined with inducible gene expression systems, so that selected candidate genes can be switched on upon addition of tetracycline or its analogue doxycycline (Tet-ON system, [37]). The advantage of this methodology is that established cell lines are genetically identical except for the absence or presence of selected candidate genes of which the expression can be controlled. In this way, highly standardized cell systems are produced.
In our experimental set-up we tested the tumor suppressor genes TP53 and PTEN, respectively, as candidate genes achieving three different cell lines: U-251MG-Ctrl (corresponds to the wild type cancer cell line; tumor suppressors TP53 and PTEN are inactivated), U-251MG-TP53 (tumor suppressor TP53 is active, PTEN is inactive), and U-251MG-PTEN (tumor suppressor PTEN is active, TP53 is inactive). Cell lines treated with the inducer doxycycline were termed "-IND" whereas non-treated cells are indicated by "-non-IND".
Resulting isogenic cell lines display different cancerous cell characteristics with U-251MG-Ctrl-(IND) expressing most malignant characteristics compared to all of the other cell lines.
All glioblastoma cell lines were cultured in DMEM supplemented with 4.5 g/l glucose, 10% fetal calf serum, 2 mM L-glutamine, 100 U $ml^{-1}$ penicillin and 100 µg $ml^{-1}$ streptomycin at 37°C in a humidified, 5% $CO_2$ environment.

- **Sample preparation.** 5 x $10^5$ cells of each cell line were seeded in 35 mm glass-bottom dishes (fluorodish, WPI, Berlin), respectively. Forty eight hours prior to measurements the expression of transgenes was induced by changing the medium to a medium containing 100 ng/ml doxycycline. For AFM experiments cells were washed twice with Hepes-buffered salt solution (HBSS) (150mM NaCl, 5 mM KCl, 1.3 mM $CaCl_2$, 1.2 mM $MgCl_2$, 10 mM HEPES, 5.6 mM glucose) and subsequently incubated in HBBS.

- **AFM:** AFM measurements were performed using a Bioscope Catalyst™ (Bruker, Billerica, USA) coupled to a DMI6000 (Leica, Mannheim, Germany) and ScanAsyst Fluid probes (Bruker, Billerica, USA). The deflection sensitivity was calibrated on a non-compliant part of the sample and the spring constant by using a thermal tune sweep, and found to be between 0.1 and 0.3 N/m.
The Young's modulus was extracted by using a Sneddon fit [38,39] which takes the deformation induced by the indenter into account, considering the AFM tip as an infinite cone, and is well adapted to biological samples. The principle of force curve processing was previously described

[36].
All the images were collected in liquid: the cells were imaged in their culture medium. For both FV and PFT experiments, the acquisition speed was 6 minutes per image and each Young's modulus value is an average of 9 measurements carried out at 3 different locations on 3 different samples, corresponding to 9214 and 589 824 force curves per condition, for force FV and PFT images respectively.

## 3. Results

FV and Peak Force Tapping (PFT) have been used to investigate mechanical properties of living isogenic glioblastoma U-251MG cells which have been genetically modified to display different levels of cancerous cell characteristics.
Figure 2 represents a typical 60x60 µm image showing glioblastoma U-251MG-TP53 cells in which the tumor suppressor TP53 is heterologously expressed.

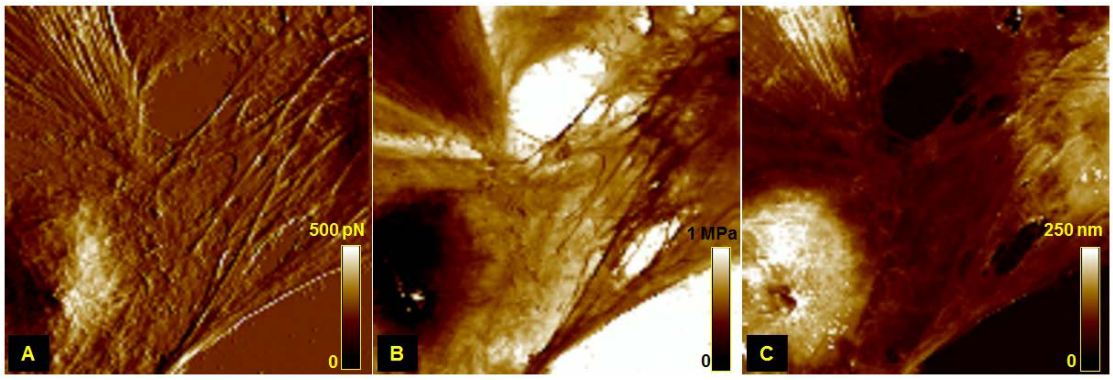


**Fig. 2.** Typical 60x60 µm images of living U-251MG glioblastoma cells with heterologous expression of the tumor suppressor TP53. Only three AFM channels are represented here: A is the Peak Force Error signal which reflects the sample's topography. B is the Young's modulus signal and C is the deformation channel. Because the information is quantitative the average elasticity and deformation values can directly be estimated. As the selected resolution is relatively low (256x256), each image can be captured in about 6 minutes. As expected, the stiffest (bright contrast on channel B) parts of the cell correspond to the less deformable areas (dark contrast on channel C) and vice versa.

In part A of figure 2 the so called peak force Error channel is illustrated which, as the amplitude channel in tapping mode or the deflection channel in contact mode, directly reflects the deflection of the cantilever while tracking the sample's surface. As the tip is calibrated to the experiment, the z-scale is directly displayed in pN instead of V. The average loading force applied to the sample was in the range of 200 pN, which is far below the usual nominal force applied when using tapping or contact modes (around 1 nN). This signal is tightly connected to the topography and several cells establishing bridges between each other can be observed. In part B of figure 2 the Young's modulus channel is shown: the brightest (stiffest) part corresponds to the glass bottom. Cells being much softer appear significantly darker on the image. A direct correlation with the left image indicates that the nucleus (clearly protruding from the rest of the cell in A) or the area above it, is much softer than the rest of the sample. The cell cytoskeleton can also be seen clearly. In part C of figure 2 the deformation channel is displayed: the contrast is inverted compared to the Young's modulus channel, stiff parts being less deformable than soft parts. For instance glass appear dark, and vice versa. Likewise to the Young's modulus channel, subcellular components, for example the nucleus

and the cytoskeleton can be identified. Simultaneously to those three signals, other channels like topography, adhesion or dissipation are also monitored but were less relevant with respect to our study, and thus not shown here. As a force curve is captured for each pixel of the image, all the channels display exactly the same number of data points. We decided to select a 256x256 resolution, since its offers a good compromise between the speed of acquisition (6 minutes per image) and a relatively high number of data points. As a comparison, a force volume image of the same resolution would have required approximately 2 hours, and being able to image the cells in a minimum of time is a key requirement. In parallel to those PFT images, FV images have also been acquired in the same time lapse (6 minutes). For such acquisition speed, getting proper tracking forced us to image at a resolution not higher than 32x32.

First in PFT mode (figure 3, blue histograms), all cell samples in which either tumor suppressors are inactivated or switched off upon absence of the inducer doxycycline [U-251MG-Ctrl glioblastoma cells treated with doxycycline (Ctrl IND), untreated U-251MG-Ctrl cells (Ctrl non-IND), non-induced U-251MG-TP53 cells (TP53 non-IND) and non-induced U-251MG-PTEN cells (PTEN non-IND)] exhibited a low Young's modulus (30.4±7.3, 38.2±5.2, 35.7±5.8 and 37.5±4.6 kPa respectively). They also exhibited a rather high deformability (155±15.9, 155±24.6, 173±17.5, 166±21.4 nm respectively) (figure 4). These data point towards enhanced malignant transformation and to a potentially high degree of invasiveness which is in agreement to the enhanced proliferation we detected in those cell lines [40].

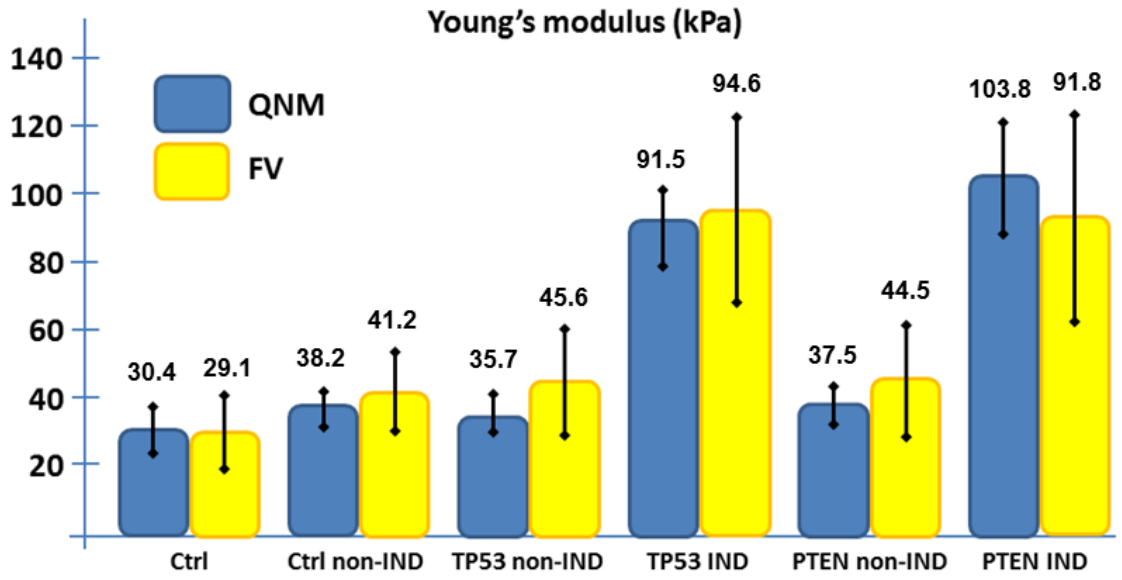


**Fig. 3.** Histogram representation of the average Young's modulus of the U-251MG glioblastoma cell lines under different experimental conditions, obtained by FV (yellow) and PFT (blue) modes. QNM, standing for Quantitative Nano-Mechanical measurements, is the quantitative version of PFT. For conditions in which the tumor suppressors are not active and thus cells display increased malignant characteristics (Ctrl cell lines and non-induced cells), the average Young's modulus is about 30 to 40 kPa. At the time cells are induced by doxycycline to express either one of the two tumor suppressors (TP53-IND and PTEN-IND), the Young's modulus is significantly increased (up to 90 to 100 kPa). Thus, the malignant state of the cell lines can be directly correlated to a spectacular change in mechanical properties. Furthermore, the approach is a well-suited methodology to determine the contribution of selected genes or their aberrant forms to a cell and disease-specific biomechanical signature.

On the contrary, cells successfully expressing either TP53 or PTEN tumor suppressors were found to be much stiffer (91.5±12.2 kPa for U-251MG-TP53-IND and 103.8±15.9 kPa for U-251MG-PTEN-IND) (figure 3, blue histograms) and less deformable (90.9±12.1 for TP53-IND and 96.2 ± 28.5 for PTEN-IND) (figure 4). Again these data are in accordance with the functions of TP53 and PTEN in cell cycle regulation and with the significant decrease of proliferation and migration rates we observed in the isogenic glioblastoma cell lines U-251MG upon induced expression of PTEN or TP53, respectively [40]. In conclusion, U-251MG cells with none of the two tumor suppressors being activated are softer by a factor of 3 compared to cells expressing either TP53 or PTEN. These findings complement previous studies in which malignant cells have been reported to be softer than their normal counterparts by factors between 2–4 [41, 42].

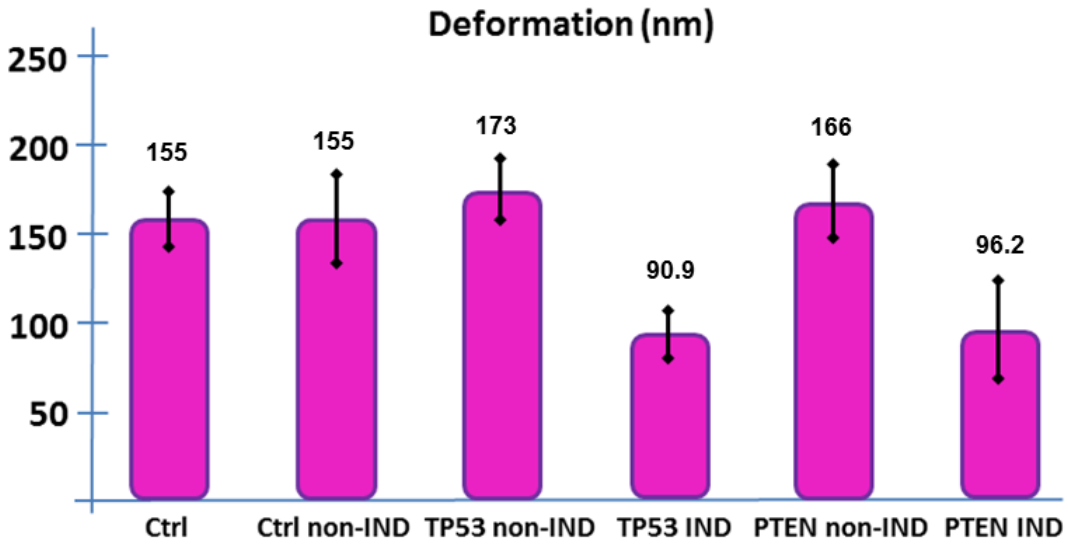


**Fig. 4.** Histogram representation of the average deformation of the glioblastoma U-251MG cells obtained by PFT mode using same conditions as described in Fig. 3. Cell deformability typically increases by a factor of two in cells (Ctrl and non-induced cells) that do not express active tumor suppressors TP53 and PTEN, respectively, in contrast to the induced counterparts in which tumor suppressors are active (IND cells). These data are in good agreement with the Young's modulus values shown in figure3.

From the FV force curves, the deformation cannot be extracted, but as with QNM force curves, the Young's modulus can directly be calculated (figure 3, yellow histograms). Cell samples in which either tumor suppressors are inactivated or switched off upon absence of the inducer doxycycline [U-251MG-Ctrl glioblastoma cells treated with doxycycline (Ctrl IND), untreated U-251MG-Ctrl cells (Ctrl non-IND), non-induced U-251MG-TP53 cells (TP53 non-IND) and non-induced U-251MG-PTEN cells (PTEN non-IND)] exhibited a low Young's modulus (29.1±11, 41.2±11.8, 45.6±15.7 and 44.5±16.5 kPa respectively). On the contrary, cells successfully expressing either TP53 or PTEN tumor suppressors were found to be much stiffer (94.6±27.1 kPa for U-251MG-TP53-IND and 91.8±30.3 kPa for U-251MG-PTEN-IND). In terms of Young's moduli, the FV results (in yellow) show exactly the same tendency as the QNM results (in blue) but the average moduli returned much higher standard deviations. In some cases (TP53 non-IND compared to TP53 induced for instance), there is an obvious cross-talking between the deviation bars and the difference between the average moduli is not significant. Those major differences in standard deviations can be explained by the significant differences in the number of data points between the two techniques. It clearly demonstrates the interest of using a technique like PFT which delivers

mechanical information at a much higher resolution, than when using a standard technique like FV.

## 4. Conclusion

Two quantitative AFM techniques, Force Volume and Peak Force Tapping were used to image different mechanical properties of living glioblastoma U-251MG cells with targeted expression of the two tumor suppressor genes TP53 or PTEN, respectively. The inactivation of tumor suppressor genes like TP53 and PTEN frequently determines the transition from a normal to a brain cancer cell, so that this scenario offers a model system for distinguishing between the healthy and the diseased state. We have shown that, combining the isogenic glioblastoma cell model and quantitative AFM measurements, significant changes in elasticity and deformation could be monitored which allowed us to discriminate between cells expressing tumor-related genes and tumor control cells. With both AFM techniques we have proven that U-251MG glioblastoma cells are about 3 times softer and 2 times more deformable in contrast to their recombinant counterparts. We showed that at a similar scan rate, Peak Force tapping measurements appeared to be much more accurate and relevant. This is mainly due to the fact that, at similar acquisition speed and because a force curve is generated at each image pixel, PFT typically provides 60 to 70 times more data points than a standard AFM technique like FV.

Building upon our results the contribution of other disease-related candidate genes to specific biomechanical properties could be investigated by AFM. Such data could potentially provide a more detailed knowledge of parameters for distinguishing between the healthy and the diseased cellular state. Furthermore, the elucidation of genotype–phenotype relationships would support further understanding of the correlation between increased elasticity and malignancy involved in disease onset and progression.

Furthermore, this study highlights the potential using Peak Force Tapping to image living cells and to quantitatively probe their mechanical properties in a relatively short time and at a high resolution. Such observations reveal the abilities of AFM methodology to serve as a potential diagnosis tool to probe cellular elasticity as a marker for the detection of cancerous lesions at an early disease stage.

### References

[1] G. Binnig, C.F. Quate and C. Gerber: Phys. Rev. Lett. **56** (1986) 930.
[2] Q. Zhong, D. Innis, K. Kjoller and V.B. Elings: Surf. Sci. Lett. **290** (1993) 688.
[3] U.G. Hofmann, C. Rotsch, W. J. Parak and M. Radmacher: J. Struct. Biol. **119** (1997) 84.
[4] K.J. Van Vliet, G. Bao, S. Suresh: Act. Mater. **51** (2003) 5881.
[5] G.Y.H. Lee and C.T. Lim: Trends Biotechnol. **25** (2007) 111.
[6] H.W. Wu, T. Kuhn and V.T. Moy: Scanning **20** (1998) 389.
[7] C. Rotsch and M. Radmacher: Biophys. J. **78** (2000) 520.
[8] I. Sokolov, S. Lyer and C.D. Woodworth: Nanomedicine **2** (2006) 31.
[9] I. Dulinska, M. Targosz, W. Strojny, M. Lekka, P. Czuba, W. Balwierz and M. Szymonski: J. Biochem. Biophys. Methods **66** (2006) 1
[10] D. Weihs, T.G. Mason and M.A. Teitell: Phys. Fluids **19** (2007) 103102.
[11] A.E. Pelling, D.W. Dawson, D.M. Carreon, J.J. Christiansen, R.R. Shen, M.A. Teitell, and J.K. Gimzewski: Nanomedicine **3** (2007) 43.
[12] C. Callies, J. Fels, I. Liashkovich, K. Kliche, P. Jeggle, K. Kusche-Virhog and H. Oberleithner: J. Cell. Sci. **124** (2011) 1936.
[13] A. Fuhrmann, J.R. Staunton, V. Nandakumar, N. Banyai, P.C. Davies and R. Ros: Phys. Biol. **8** (2011) 015007.
[14] H. Yamaguchi and J. Condeelis: Biochim. Biophys. Acta 1773 (2007) 642.
[15] I. Ramis-Conde, D. Draso, M.A.J. Chaplain and A.R.A. Anderson, : Biophys. J. 95 (2008) 155.
[16] E. Canetta, M. Mazilu, A. De Luca, A. Carruthers, K. Dholakia, S. Neilson and H. Sargeant: Biorheology

**42** (2005) 321.
[17] B. Chen, Q. Wang and L. Han: Scanning **4** (2004) 162.
[18] Q. Li, G.Y.H. Lee, C.N. Ong and C.T Lim: Biochem. Biophes. Res. Commun. **374** (2008) 609.
[19] S. Morreno-Flores, R. Benitez, M. Vivanco and J.L. Toca-Herrera: Nanotechnology 44 (2010) 445101.
[20] E.C. Faria, N. Ma, E. Gazi, P. Gardner, M. Brown, N.W. Clarke and R.D. Snook : Analyst **133** (2008) 1498.
[21] X. Cai, X. Xing, J. Cai, Q. Chen, S. Wu and F. Huang: Micron **41** (2010) 257.
[22] M. Li, L. Liu, N. Xi, Y. Wang, Z. Dong, O. Tabata, X. Xiao and W. Zhang: Biochem. Biophys. Res. Commun. **404** (2011) 689.
[23] M. Lekka, P. Laidler, D. Gil, J. Lekki, Z. Stachura, and A. Z. Hrynkiewicz: Biophys. J. 28 (1999) 312.
[24] S.E. Cross, Y.S. Jin, J.Y. Rao and J.K. Gimzewski: Nanotechnol. **2** (2007) 780.
[25] E.M. Darling, S. Zauscher, J. A. Block, and F. Guilak: Biophys. J. 92 (2007) 1784.
[26] M.J. Rosenbluth, W.A. Lam and D.A. Fletcher: Biophys. J. **90** (2006) 2994.
[27] S. Sharma, C. Santiskulvong, L.A. Bentolila, J.Y. Rao, O. Dorigo and J.K Gimzewski: Nanomed. Namotechnol. Biol. Med. **5** (2012) 757.
[28] A.N. Ketene, E.M. Schmelz, P.C. Roberts and M. Agah: Nanomed. Namotechnol. Biol. Med. **8** (2012) 93.
[29] M. Lekka and P. Laidler, Nat. Nanotechnol. **72** (2009) 72.
[30] J. Hertz: *für reine und angewandte Mathematik* **92** (1881) 156.
[31] M. Khasraw and A.B. Lassman: Curr. Oncol. Rep. **12** (2010) 26.
[32] R.Y. Bai, V. Staedtke and G.J. Riggins: Trends Molec. Med. **17** (2011) 301.
[33] J. Adamcik, A. Berquand and R. Mezzenga : Appl. Phys. Lett. **98** (2011) 193701.
[34] A. Berquand, C. Roduit, S. Kasas, A. Holloschi, L. Ponce and M. Hafner : Microscopy Today **6** (2010) 24.
[35] G. Pletikapic, A. Berquand, T. Misic-Radic and V. Svetlitic: J. Phycol. **48** (2012) 174.
[36] C. Heu, A. Berquand, C. Caille-Elie and L. Nicod ; J. Struct Biol. **178** (2012) 1.
[37] M. Gossen, S. Freundlieb, G. Bender, W. Hillen and H. Bujard : Science **268** (1995) 1776.
[38] I.N. Sneddon: Int. J. Eng. Sci. **3** (1965) 1.
[39] S. Belikov, N. Erina, L. Huang, C. Su, C. Prater, S. Magonov, V. Ginzburg, B. McIntyre, H. Lakrout and G. Meyers: J. Vac. Sci. Technol. B **27** (2009) 47.
[40] A. Holloschi, H.M. Kuhn, C. Müller, M. Worf, M. Rauen, T. Röder, W. Kessler, J. Mollenhauer and P. Kioschis: Curr. Micr. Contr. Adv. Sci. Technol. **1** (2012) 103.
[41] Q.S. Li, G.Y.H. Lee, C.N. Ong, C.T. Lim: Biochem. Biophys. Res. Comm. **374** (2008) 609.
[42] A. Fuhrmann, J. R. Staunton, V. Nandakumar, N. Banyai1, P. C. W. Davie and R. Ros: Phys Biol. **8** (2011) 015007.